UNCLASSIFIED

ATI 134 070 (COPIES OBTAINABLE FROM ASTIA-DSC)

PRINCETON UNIVERSITY, AERONAUTICAL ENGINEERING LAB., N.J.
(REPORT NO. 184)

A PRELIMINARY INVESTIGATION OF A SHOCKWAVE-TURBULENT
BOUNDARY LAYER INTERACTION

BOGDONOFF, S.M.; SOLARSKI, A.H. 30 NOV'51 36PP PHOTOS,
GRAPHS, DRWG

USN CONTR. NO. N6-ORI-270

BOUNDARY LAYER - EFFECT OF SHOCK WAVES
BOUNDARY LAYER, TURBULENT
BOUNDARY LAYER - VELOCITY DISTRIBUTION
SHOCK WAVES

AERODYNAMICS (2)
BOUNDARY LAYER (5)

UNCLASSIFIED

A PRELIMINARY INVESTIGATION OF A SHOCKWAVE - TURBULENT BOUNDARY LAYER INTERACTION

BY

S. M. BOGDONOFF

AND

A. H. SOLARSKI

PRINCETON UNIVERSITY

AERONAUTICAL ENGINEERING LABORATORY

Report No. 184

Nov. 30, 1951

UNITED STATES NAVY

Office of Naval Research
Mechanics Branch, Mathematical Sciences Division

and

UNITED STATES AIR FORCE

Office of Air Research

(Contract N6-ori-270, Task Order No. 6,

Project Number NR 061-049)

A PRELIMINARY INVESTIGATION OF A SHOCK WAVE-TURBULENT BOUNDARY LAYER INTERACTION

By

S. M. Bogdonoff and A. H. Solarski

PRINCETON UNIVERSITY

AERONAUTICAL ENGINEERING LABORATORY

Report No. 184

November 30, 1951

ACKNOWLEDGEMENT

The [illegible] is part of a program of theoretical and experimental [illegible] interaction effects in supersonic flow being [illegible] Engineering, Princeton University. This research was sponsored jointly by the Office of Naval Research (U.S.N.), Mechanics Branch, Mathematical Sciences [illegible] and by the Office of Air Research (U.S.A.F.).

The authors wish to express their appreciation for the many interesting discussions held with Professors Lees and Crocco. Their work on the theoretical solution of the shock wave boundary layer problem has provided an added stimulus to the experimental research.

TABLE OF CONTENTS

SUMMARY

Preliminary data in the form of static and pitot pressure distributions and shadow and Schlieren photographs have been obtained for the interaction of a pressure ratio 2.09 shockwave with a turbulent boundary layer on a flat wall at M = 2.97. Separation of the boundary layer appears to be incipient and a model of the interaction has been constructed. The model is similar to that of Bardsley and Mair for turbulent layer-medium strength shocks and resembles as well that obtained by Liepmann for the interaction of weak shocks with a laminar layer at low Mach numbers. Longitudinal static pressure distributions show an upstream influence of approximately three boundary layer thicknesses with an inflection in the curve characteristic of laminar interactions. The entire pressure rise occupies six boundary layer thicknesses and agrees satisfactorily with the theoretically predicted rise. Velocity profiles in the region of the steepest pressure rise, i.e., slightly ahead of the point of impingement of the incident shock, show a behavior that may be associated with imminent separation. Downstream of this point, the boundary layer profiles are similar to those measured in an adverse pressure gradient. Although the pressure after the interaction was constant, the boundary layer profile had not returned to the normal turbulent profile two boundary layer thicknesses downstream of the interaction region.

Tests of two wedges of different widths showed a very large "relieving" effect for the wedge which did not completely span the tunnel. The erroneous results obtained with the narrow wedge may explain some of the discrepancies in the existing data.

A PRELIMINARY INVESTIGATION OF A SHOCK WAVE-TURBULENT BOUNDARY LAYER INTERACTION

INTRODUCTION:

The phenomenon of the interaction of a shock wave with the boundary layer on a flat plate has received considerable attention in the last few years. An understanding of this fundamental simplified interaction is an essential preliminary step to the study of the more complicated interaction, as, for example, the shock wave-boundary layer interactions at wing trailing edges, around deflected control surfaces, at wing-body junctures, and in supersonic diffusors and compressors. The effects of the interaction may extend some distance along the wall and may influence the external flow to a large extent, in contradiction to the theoretical non-viscous case of a shock wave impinging on a solid wall.

The work of Leipmann[1] and others[2] on laminar layers has provided information on the extent of the pressure field on the solid wall and a general model of the interaction has been constructed. The incident shock wave is reflected as an expansion wave with a slow compression region appearing ahead of the point of impingement due to separation or thickening of the boundary layer. Behind the point of impingement there is another region of slow compression where the flow re-attaches to the surface. The upstream compression, reflected expansion, and downstream compression coalesce far from the wall to give a single shock wave close to that predicted for the non-viscous shock reflection. The effects of shock wave strength and Reynolds number have been studied at Mach numbers of two and lower. Theoretical work[3] has been able to predict roughly the upstream influence of the interaction, but the problem of predicting the separation point and the reattachment of the laminar boundary layer has not yet been solved.

The interaction of a shock wave with a turbulent boundary layer has also been studied. Several of the investigators[1,2] who studied laminar layers, "tripped" the boundary layer near the leading edge of the plate and obtained some preliminary results. Bardsley and Mair[4] at a Mach number of two, made an excellent set of Schlieren photographs of the interaction of varying strength oblique shock waves with a turbulent boundary layer on the tunnel wall. Weak incident waves are reflected as a compression (an oblique shock wave) followed by a narrow expansion region which is followed by a slow compression region. No separation is noticed. For higher shock strength, the flow separated at the wall and the first reflected compression moved upstream of the point of impingement of the incident shock. The reflection was still a compression, expansion, and slow compression which agrees with the general interaction picture found for the laminar layer. The scale of the interaction region, i.e. the influence of a given strength shock is, of course, quite different. The most complete results available are those of Fage and Sargent[5]. Their results were obtained at Mach numbers from 1.2 to 1.6 and are primarily on shocks which reflect as Mach shocks (normal shocks) near the wall.

In an effort to get a better understanding of the shock wave-turbulent boundary layer interaction, and to provide the detailed data needed to build a correct theoretical model, a series of tests have been undertaken at the Supersonics Laboratory of the Aeronautical Engineering Department of Princeton University. The program will cover a range of

Mach numbers from about 2.5 to 4.0 for turbulent boundary layers interacting with shock waves of varying strength. The data presented herein are the first preliminary results obtained at a Mach number of 3 with a shock wave of about a pressure ratio of 2.

Concurrent with the reported experimental studies, Professors Lees and Crocco have been carrying on an extensive theoretical study of the shock wave-turbulent boundary layer interaction. Their results and comparison with the experimental work will be presented in a later paper.

EXPERIMENTAL EQUIPMENT:

The tests were performed in the Princeton Pilot Supersonic Tunnel which has been modified in several details since [illegible] constructed. Test section size has been increased to 2" wide by 2-1/2" high. Additional air storage capacity, 170 cu. ft. as compared to 50 cu. ft. now permits longer running times than before.

The boundary layer on the tunnel wall was utilized for the measurements. Two 10° shock producing wedges were employed which differed in width and length, the narrower one being 1-1/4" wide and 2-1/8" long and the other nearly 2" wide and 2-7/16" long. The wider wedge spanned the tunnel to within .010" of either side wall. Both wedges had a .030" static pressure orifice drilled on centerline 1/2" from the leading edge, and the wider one a similar orifice drilled 1" from the leading edge. The pressure ratio of the shock was determined by using these static pressures rather than the geometrical wedge angle, thus taking into account any effect of the boundary layer on the wedge.

For measuring the static pressure on the interacting surface, a .030" orifice drilled in the nozzle block was selected and the shock generator set up in such a way as to allow the shock to pass over the orifice as the wedge was moved axially in the tunnel. Static pressures spanwise at this station were also recorded in order to check the two-dimensionality of the shock interaction. These were located 3/8", 1/2", 5/8" and 3/4" off axis. A micrometer drive was devised for movement of the wedge which allowed setting to within a thousandth of an inch. Readings were taken in the interaction region every tenth of an inch relative to the shock position. An arbitrary zero was selected as a reference, positions ahead being labeled "minus", and positions behind "plus".

Boundary layer total pressure surveys normal to the wall were made at several stations in the interaction region, those furthest ahead being out of the region of influence of the shock and those furthest behind being in a uniform region after the interaction. A carefully made total-head tube was employed which permitted readings to within .004" of the surface. The tube was constructed of .065" O.D. steel tubing flattened at the end for about 3/4" and honed on the bottom surface to allow close approach to the wall. The orifice becomes a slit about .004" high by .060" wide; a sketch is given below.

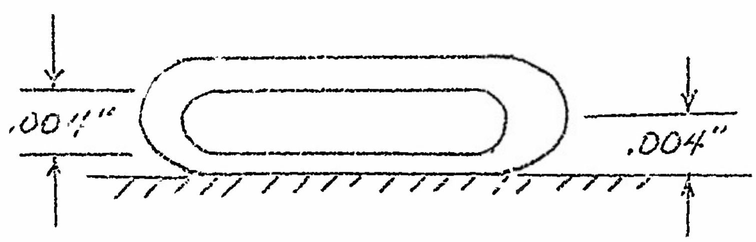

Lateral checks were made with total head surveys 1/4" and 1/2" off the tunnel axis using probes of identical geometry as that for the centerline case.

Fig. 1 shows all the components of the experimental setup.

SYMBOLS :

x	distance along tunnel wall, inches.
y	distance normal to tunnel wall, inches.
P_o	original stagnation pressure of flow.
P_3	pitot pressure, stagnation pressure behind normal shock.
P_1	static pressure as measured along tunnel wall.
P_2	static pressure behind oblique shock.
Δ	deflection of flow in degrees caused by shock wave of strength characterized by Δ .
δ	boundary layer thickness, inches.
δ^*	boundary layer displacement thickness.
Θ	boundary layer momentum thickness.
H	boundary layer form parameter δ^*/Θ

RESULTS AND DISCUSSION:

The investigation was begun using the "narrow" shock generator, the first determination being that of static pressure variation along the wall, on centerline, in the region of the interaction. It was immediately noticed that the static pressure rise after the shock, which for the reflection of an approximate 10^o wave should have a value of about 3.8, was far short of that amount. A shadowgraph, Fig. 2, and a Schlieren photograph, Fig. 3, are presented together with a sketch of the interaction, Fig. 4, as traced from the Schlieren picture. Corresponding to the sketch is a curve showing the static pressure variation throughout the interaction. All the pressure rise for this case is accomplished in about 2-1/2 boundary thicknesses, and the curve is smooth. The pressure ratio across the shock, about two as measured by means of the orifice on the wedge, calls for the overall pressure rise at the wall to about 3.8 whereas the measured rise is only 2.5. No uniform region appears ahead of the expansion fan from the wedge corner. The photographs show a reflection that appears approximately regular, no boundary layer separation occurring.

Evidently there must exist a considerable "relieving effect" due to the three-dimensional character of the flow around the edges of the shock generator. When, later, additional orifices were drilled laterally in the nozzle block, the non-uniformity of the interaction became quite apparent. Fig. 5 gives the cross-wise pressure distributions for several shock positions and illustrates how the low external pressure affects the interaction region.

Further tests with the narrow wedge were discontinued, but it is planned to examine the problem later using a series of wedges of varying widths to determine if possible the range of this three-dimensional behavior. It is suggested that the three-dimensional effects that are introduced by using a shock generator of insufficient width may be responsible for Leipmann's results for the turbulent case. For a shock wave of 3° at $M = 1.4$ Leipmann obtained the theoretical pressure rise, but for an increased strength shock of $4\text{-}1/2^{\circ}$, the pressure is considerably lower than theoretical. Similar results are shown by Fage and Sargent with some curves showing only half the theoretical rise. An accurate picture, therefore, of the interaction problem for a flat plate must be based upon test results that are truly two-dimensional, and future experiments should be performed in the light of this fact.

In an attempt to eliminate three-dimensional effects, a new series of test were run using the full-span shock generator. A shadowgraph, Fig. 6, a Schlieren photograph, Fig. 7, and the static pressure variation through the interaction in juxtaposition with a sketch of the interaction, Fig. 8, show immediately the differences between this and the "narrow" case. The first reflected compression has moved forward so as to intersect the incident shock approximately at the edge of the boundary layer. A thin line, resembling that seen for a separated region, appears embedded in the boundary layer adjacent to the wall between stations -.5 and -.1. The static pressure variation through the interaction has an inflection and is spread out to about six boundary layer thicknesses, with the influence being felt only a few thicknesses ahead of the point of impingement. The pressure rise begins at about station -.6, which from the picture is the point where the first reflected compression originates. A uniform region after the interaction, beginning about station +.5, appears between the second set of compression waves and the expansion fan from the wedge corner.

The model for the interaction is approximately as follows: The first reflected compression originates at a point a couple of boundary layer thicknesses ahead of the point of impingement of the incident shock. Immediately after its intersection with this reflected wave the incident shock curves sharply downward toward the wall, terminating at a point which is the apex of a small separated (probably) region. This separation appears to begin at the point of origin of the first reflected compression, and re-attachment occurs in about three boundary layer thicknesses. An expansion fan caused by the curvature of the incident shock near the wall follows the first reflected compression. Finally there is a well spread out region of slower compression waves which coalesce into a second reflected shock. This model agrees closely with that given by Bardsley and Mair[4] for interactions of medium strength shocks with turbulent boundary layers.

The static pressure rise agrees with that given theoretically within the limits of experimental accuracy. The shock pressure ratio as given by the forward wedge orifice is 2.09, while the ratio given by the rearward orifice is 2.07. These limits define the range of accuracy of the measurements. The Mach number ahead of the shock has been taken for these calculations to be 2.97, but tunnel characteristics indicate a Mach number variation of $\pm$.03 along the test section which should be taken into account. A. Ferri has pointed out that there are reflected waves caused by interactions of the several parts of the original reflected wave system. These reflected waves would be sent out until the original reflected wave system coalesced into a single shock. Since this did not occur in the dimensions of the experiment it would be expected that a small further pressure increase would occur if the tunnel were larger. Since this increase in pressure is quite small, however, its effects should not influence the results obtained. Two-dimensionality of the interaction is substantiated by the readings of the lateral orifices, Fig. 9, for several relative shock positions.

A longitudinal plot of the total pressure variation through the interaction at a point .004" from the wall is presented in Fig. 10. The rise occupies approximately the same interval as does the static pressure rise at the wall. Data at station -.7 is probably influenced by some non-uniformity of the flow in the tunnel, which may account for certain otherwise unexplained deviations in some of the parameters calculated for that station.

Velocity profiles computed on the basis of constant stagnation temperature in the boundary layer are given for several stations in the interaction region. The assumption of constant static pressure through the layer is made, using the value at the wall as given in Fig. 8. This pressure, p_1. together with the measured total pressure, P_3, gives from the Rayleigh Pitot Equation the Mach number distribution in the boundary layer. Evidently this method is accurate only near the wall since away from the wall the complicated shock system invalidates the assumption of constant static pressure. Difficulty arises in choosing a reference velocity, U_1, at the boundary layer edge. One may examine the total pressure profiles through the boundary layer and thereby determine approximately the point where they tend to level off, calling that point the edge of the boundary layer. The pressure, P_3, at that point referred to the original stagnation pressure, P_o (assumed constant through the interaction) gives the Mach number, M_1, at the boundary layer edge. Alternatively, M_1 may be calculated from the isentropic relation using the local wall static pressure, p_1, and the original stagnation, P_o. The latter has been adopted in this report as being the more convenient and eliminating the guesswork involved in determining the edge of the boundary layer from complicated total pressure surveys. The former method is illustrated in this report in two profiles, Figs. 12 and 14 to serve as a basis of comparison with the method which has been adopted.

Profiles for the region after the shock have also been computed on the basis of total head losses as calculated for the case of regular reflection from a wall with no boundary layer. A total head loss of six percent exists in this hypothetical case, but in the real case it is somewhat less due to the region of slow compression which replaces the single reflected shock of "regular" reflection. A single case, the profile at station /1.0, is presented for comparison with the profile as calculated by the method adopted for this report.

Examination of the profiles presented indicates from Figs. 11 and 12, stations -1.0 and -.7, that the boundary layer is essentially turbulent in character in the region of the interaction. The Reynolds number based on momentum thickness for the station just ahead of the interaction region is 7500. A profile calculated from the 1/7th power is presented in Fig. 11 for comparison with the experimental profile.

Beginning at station -.6 and continuing through -.1, Figs. 13 through 16, the profiles have somewhat the appearance of profiles in a separated region. However, instead of going to zero or negative velocities at the wall -- in the manner of a separated profile -- the profiles show a considerable region of high Mach number subsonic flow. These profiles may be the transition in supersonic flow from the usual turbulent profile to the detached profile, i.e. separation will occur for a wave of slightly higher strength. Further tests employing varying shock strengths will indicate whether this premise is correct.

Referring to the Schlieren photograph and the pictorial, Figs. 7 and 8, it is seen that the thin line resembling separation of the boundary layer appears almost precisely for the stations giving the disturbed profiles described above. Further, the static pressure distribution shows an inflection in the neighborhood of station -.1 where the last of these disturbed profiles is observed.

For stations +.1 through +.5, Figs. 17 through 19, the profiles are typical of turbulent profiles in an adverse pressure gradient. These correspond to the region of slow compression which appears in the Schlieren photograph, Fig. 7, and in the static pressure distribution beyond the point of inflection of the curve. Stations +.7, +1.0, and +1.3 have increasingly fuller profiles, and indicate completion of the interaction and a trend towards the characteristic undisturbed turbulent boundary layer. Although the region of constant static pressure after the interaction is approximately 3 boundary thicknesses in length, the full turbulent profile is not yet re-established.

Curves of δ, δ^*, Θ and H versus position are shown in Figs. 23 and 24. The values shown have been calculated by (1) assuming no shock wave losses and (2) assuming shock losses calculated for theoretical regular reflection without boundary layer. The difference between values calculated by both methods is not large and the general trends shown should be correct. Data close to the point of impingement of the shock (Station -3) shows erratic behavior. This is to be expected in light of the odd profile obtained when the shock wave comes close to the wall. It is interesting to note that the values for H before and after the interaction are in general agreement with Wilson's[7] formula for H as a function of Mach Number.

A comparison was made of the results described herein with those obtained by other investigators. The data on turbulent boundary layers[1,2] shows a very steep but smooth rise in pressure for all cases tested. However, the results are all for weaker strength shocks and lower Mach numbers than used in these tests. The present work shows a definite inflection point in the pressure rise curve, Fig. 8 similar to that experienced for laminar layers. It seems likely, therefore, that the difference between the laminar and turbulent interactions may be merely a difference in the shock pressure ratio required for separation. The data obtained is very similar to that for a laminar layer interacting with a very weak wave. Extension of the present work to varying shock strengths is needed to substantiate this premise.

CONCLUSIONS:

The detailed static and pitot surveys through the shock wave-turbulent boundary layer interaction have resulted in the following conclusions:

1) For the type of experiment performed, it is necessary for the shock generator to completely span the tunnel. The narrow wedge gave erroneous results which may explain some of the discrepancies in the existing data.

2) For the one interaction investigated, a shock wave of pressure ratio 2.09 interacting with a turbulent boundary layer at $M = 2.97$, separation appears imminent. The model of the interaction agrees well with that of Bardsley and Mair[4] for medium shock strength-turbulent layer interaction. It resembles, as well, that obtained by Leipmann[1] for the interaction of a weak shock with a laminar layer at low Mach numbers.

3) Static pressure distributions on the wall show an upstream influence of approximately three boundary layer thicknesses with the entire interaction taking about six boundary layer thicknesses.

4) The pressure rise curve shows an inflection point which coincides with what seems to be a small separated region noticeable in the Schlieren photographs. Ahead of this region, the pitot surveys show profiles somewhat similar to those obtained in a separated flow. Behind this region, the profile changes to one associated with flow in an adverse pressure gradient.

5) Two boundary layer thicknesses downstream of the completed interaction, the boundary layer has not yet returned to the normal turbulent profile.

6) This preliminary investigation provides a detailed picture of the interaction not heretofore available. Continued research for varying strength shock waves at several Mach numbers is to be carried out in an attempt to detail the interaction over a wide range. Such data is needed to completely understand the mechanism of interaction and to provide the basis for a fundamental theoretical study.

REFERENCES

1) Liepmann, H.W., Roshko, A. and Dhawan, S.: On the Reflection of Shock Waves from Boundary Layers. NACA TN 2334 April 1951.

2) Barry, F.W., Shapiro, A.H., and Newmann, E.P.: The Interaction of Shock Waves with Boundary Layers on a Flat Surface. Meteor Report No. 52, Massachusetts Institute of Technology. March 1950.

3) Lees, L.: Interaction Between the Laminar Boundary Layer over a Plane Surface and an Incident Oblique Shock Wave. Aeronautical Engineering Laboratory Report No. 143. Princeton University. January 24, 1949.

4) Bardsley, O. and Mair, W.A.: The Interaction Between an Oblique Shock Wave and a Turbulent Boundary Layer. Philosophical Magazine, Ser. 7, Vol. 42, page 29. Jan. 1951.

5) Fage, A. and Sargent, R.E.: Shock Wave and Boundary Layer Phenomena near a Flat Surface. Proceedings of the Royal Society. Vol. 190, S Series A. No. 1020, p. 1-20, June 17, 1947.

6) Bogdonoff, S.M.: The Princeton Pilot Variable Density Supersonic Wind Tunnel. U.S.N. Project Squid, Technical Memorandum No. PR-8. Princeton University, May 29, 1948.

7) Wilson, Robert E.: Turbulent Boundary Layer Characteristics at Supersonic Speeds -- Theory and Experiment. Journal of the Aeronautical Sciences, September 1950.

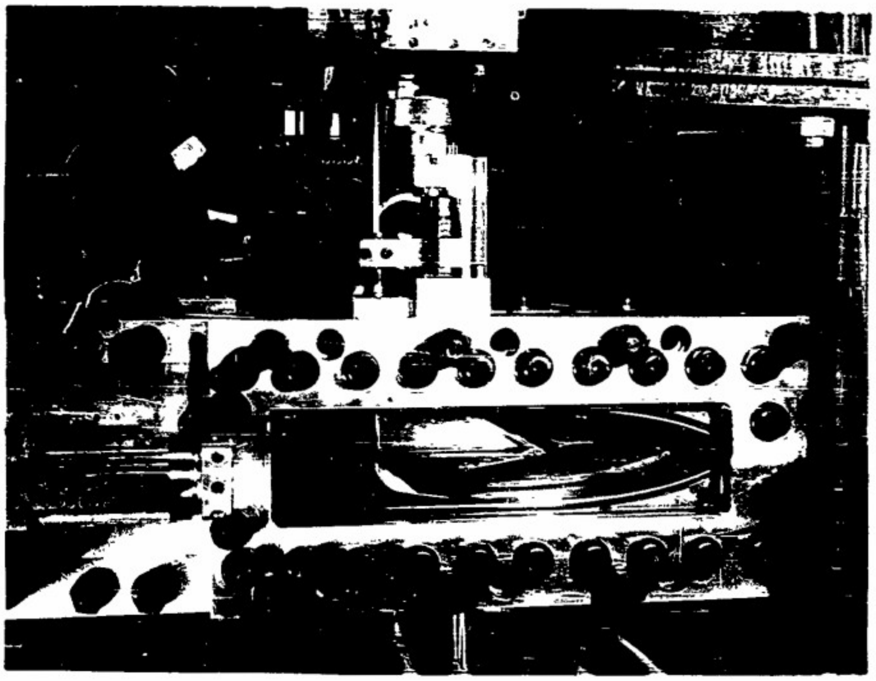

Fig. 1. Experimental Setup showing shock generator, total head probe, and micrometer drive systems for wedge and probe.

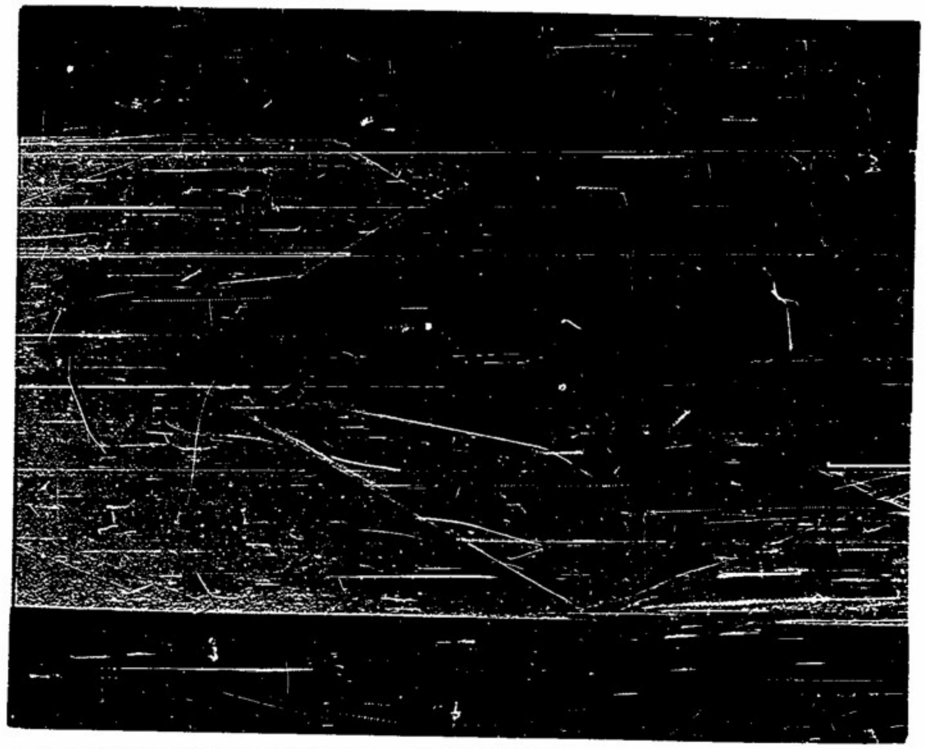

Fig. 2. Shadowgraph of interaction. (Narrow wedge)

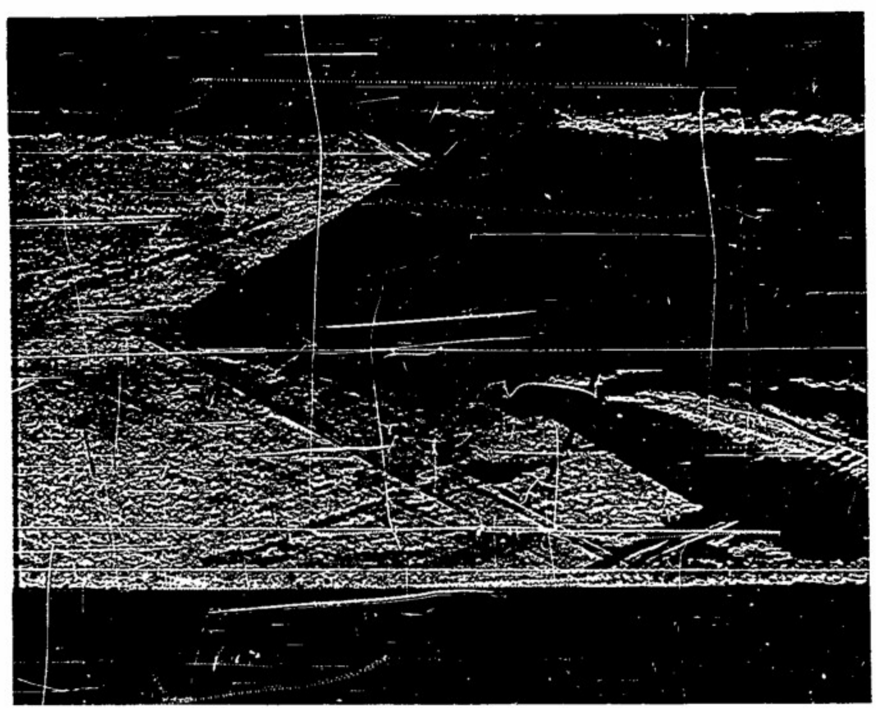

Fig. 3. Schlieren photograph of interaction. (Narrow wedge)

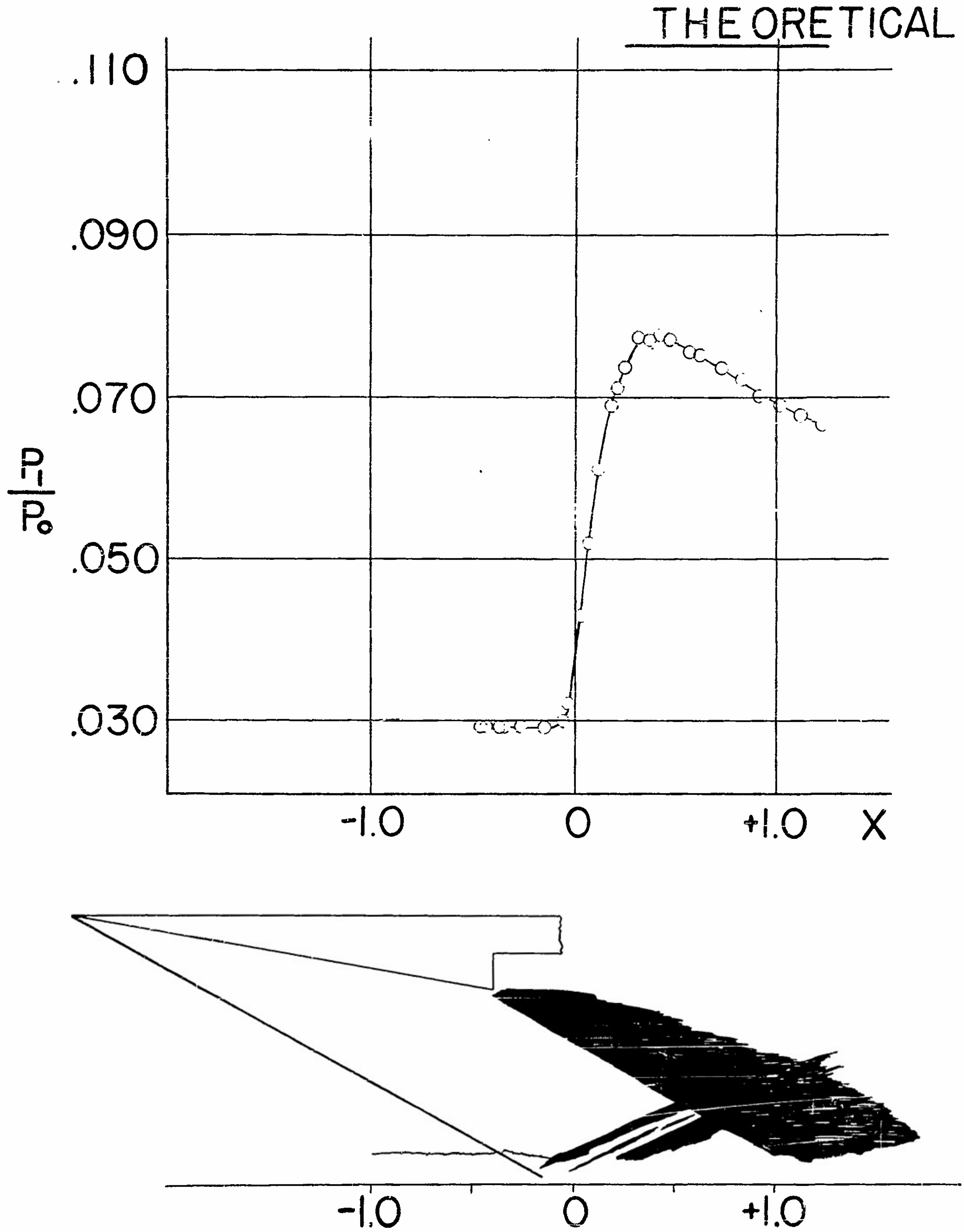

FIG. 4 SKETCH OF INTERACTION WITH VARIATION OF WALL STATIC PRESSURE —— NARROW WEDGE

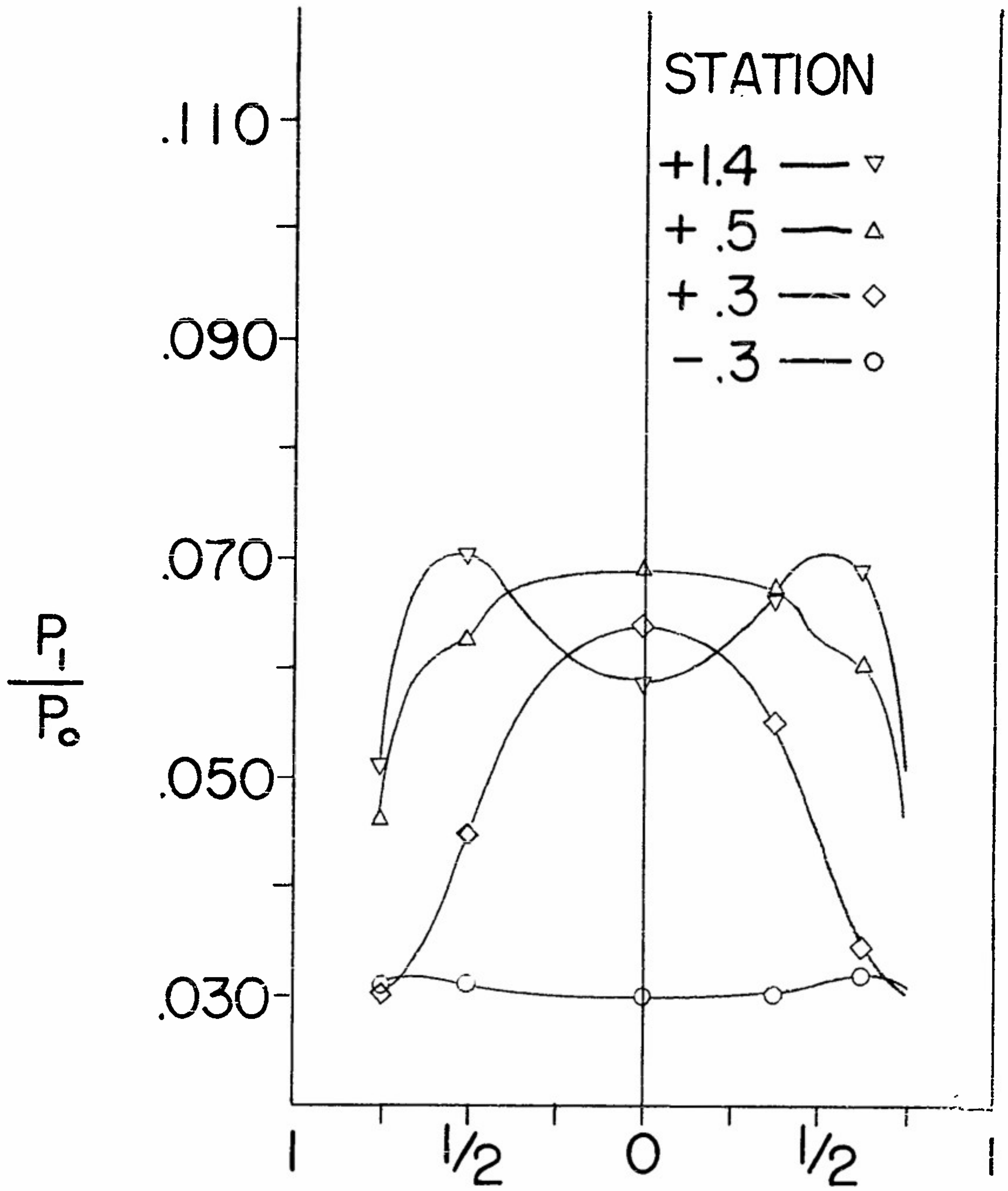

FIG. 5 SPANWISE STATIC PRESSURE DISTRIBUTION FOR SEVERAL SHOCK POSITIONS — NARROW WEDGE

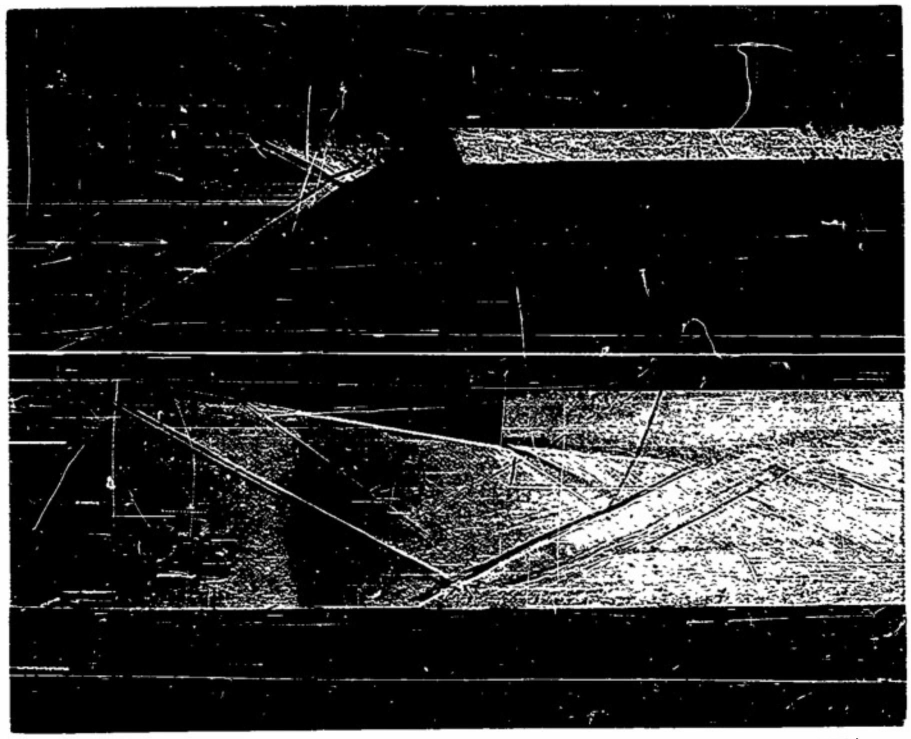

Fig 6 Shadowgraph of interaction. (Full-span wedge)

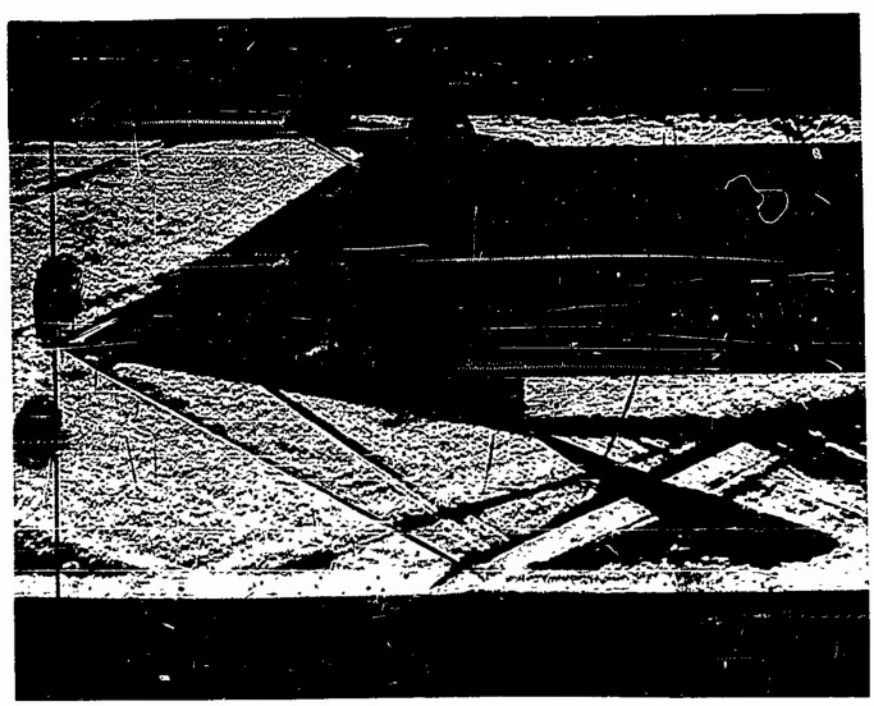

Fig 7 Schlieren photograph of interaction. (Full-span wedge)

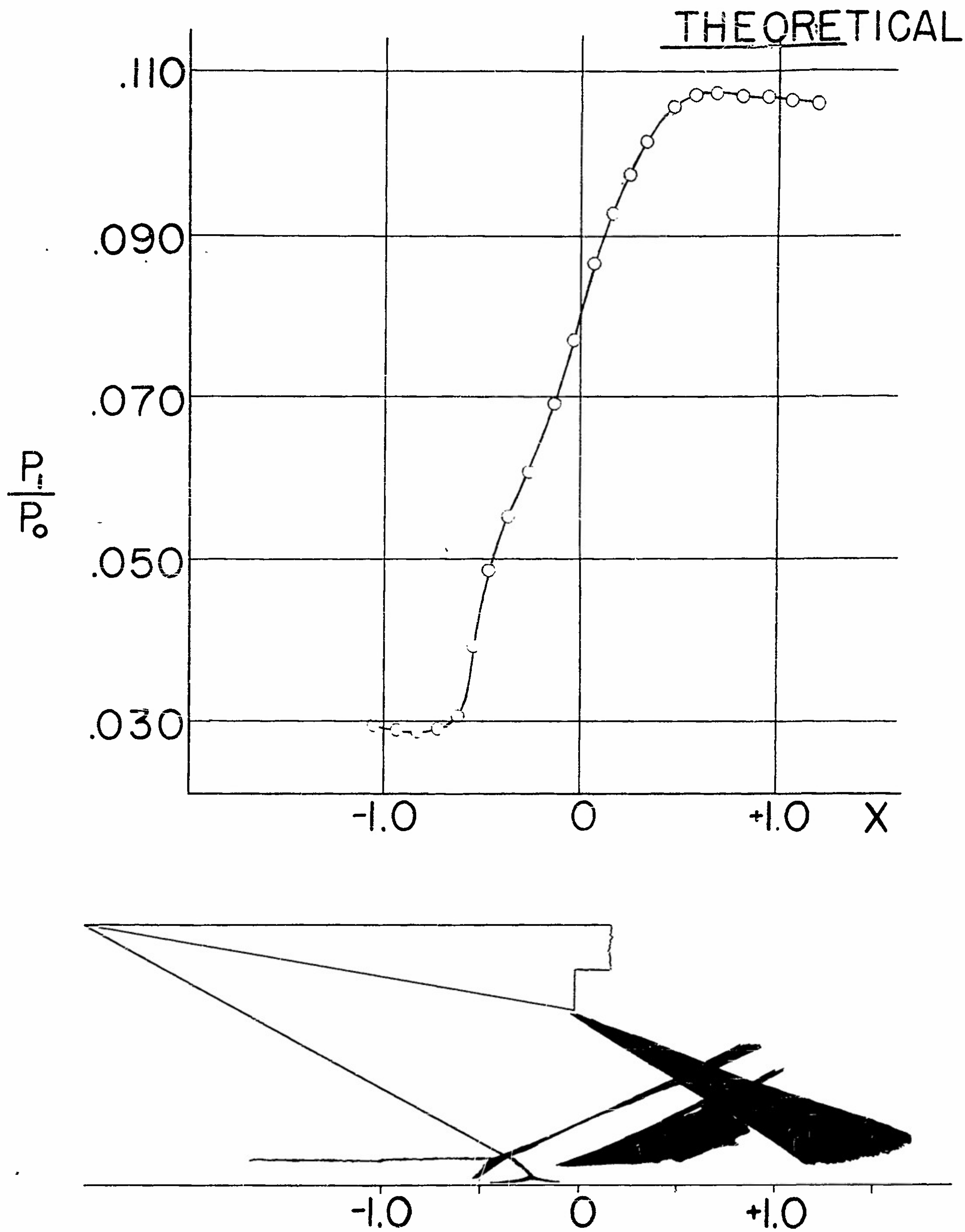

FIG. 8 SKETCH OF INTERACTION WITH VARIATION OF WALL STATIC PRESSURE — FULL SPAN WEDGE

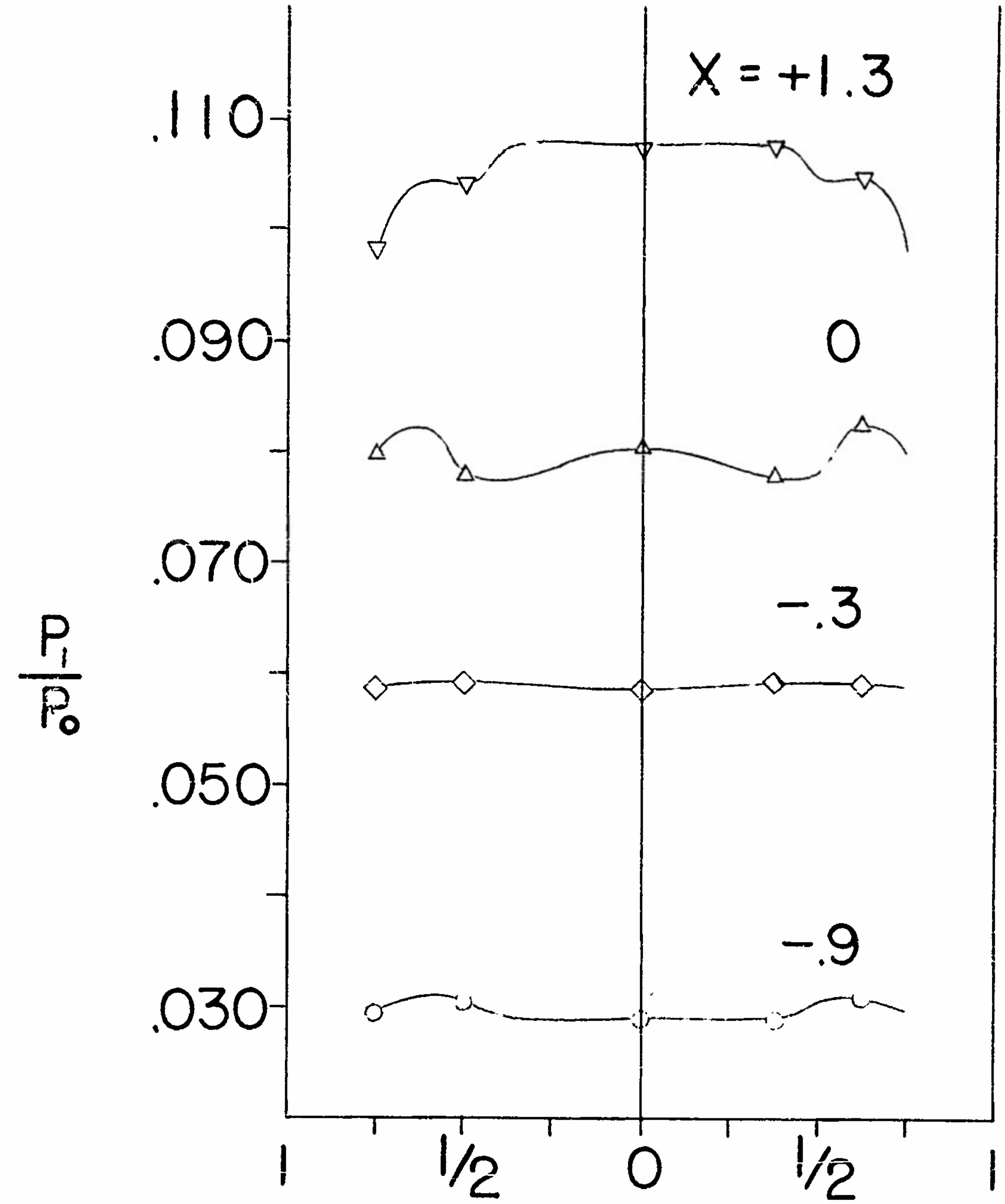

FIG. 9 SPANWISE STATIC PRESSURE DISTRIBUTION FOR SEVERAL SHOCK POSITIONS — FULL-SPAN WEDGE

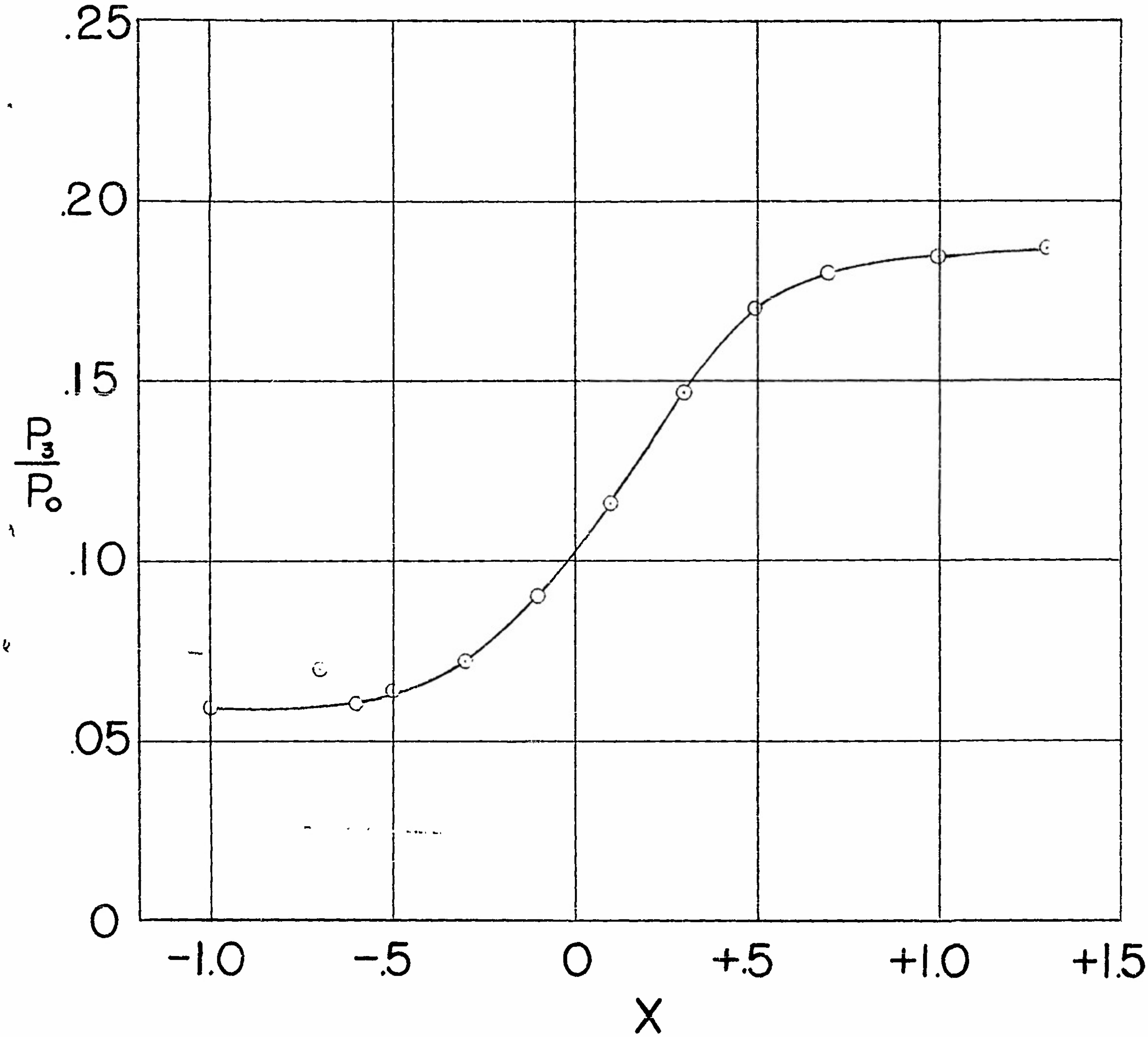

FIG. 10 VARIATION OF PITOT HEAD THROUGH INTERACTION AT Y = .004

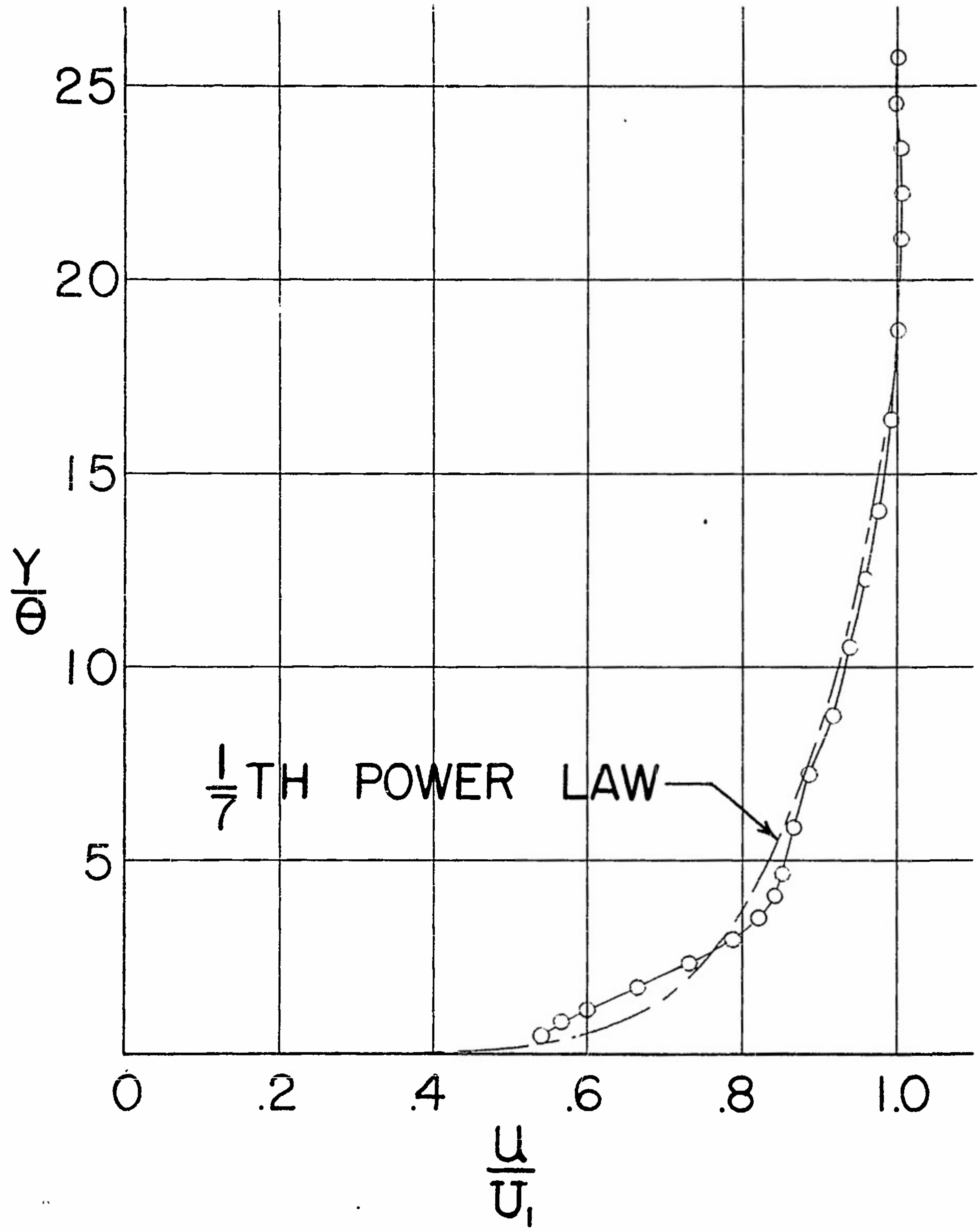

FIG. 11 VELOCITY PROFILE AT STATION -1.0

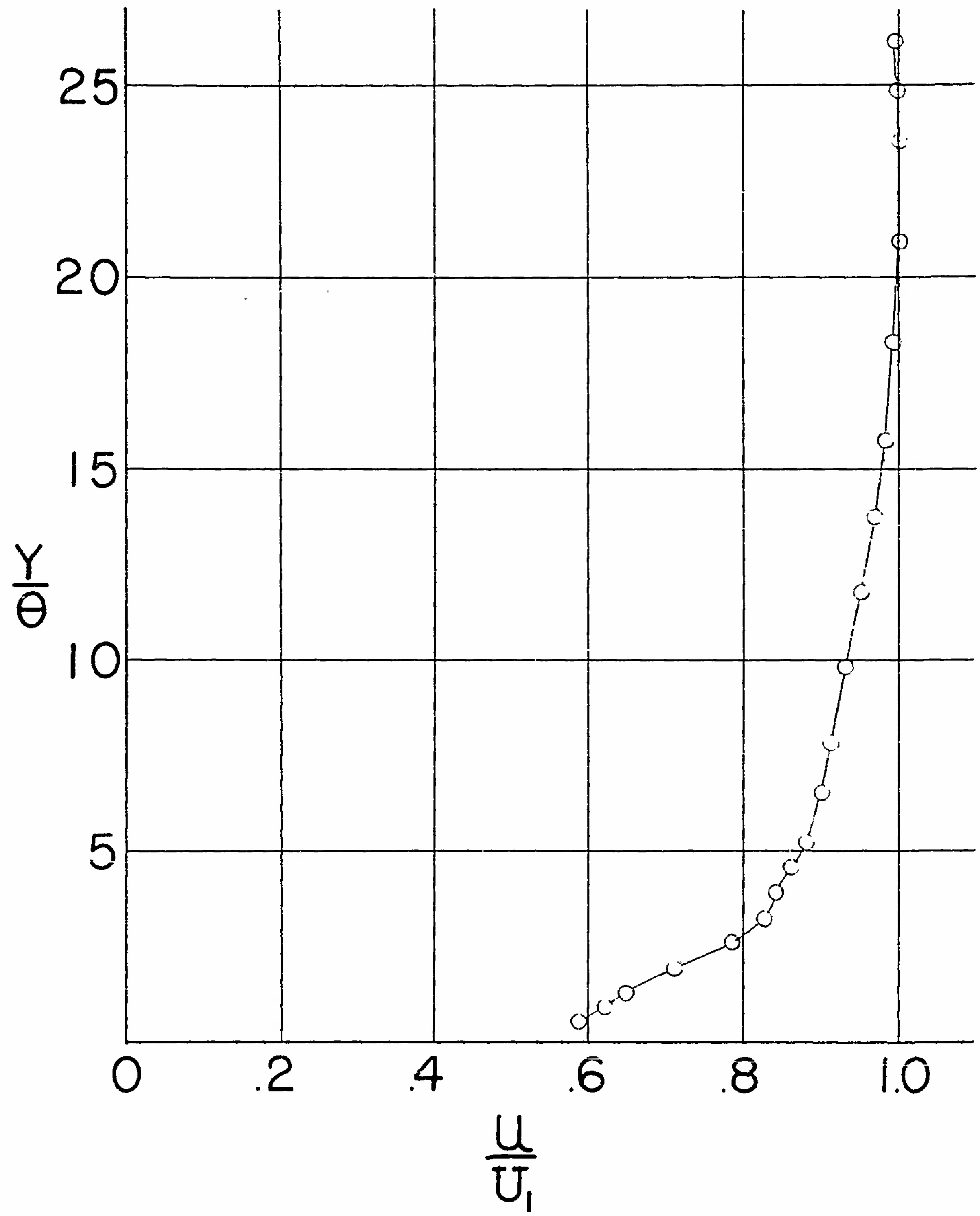

FIG. 12 VELOCITY PROFILE AT STATION -.7

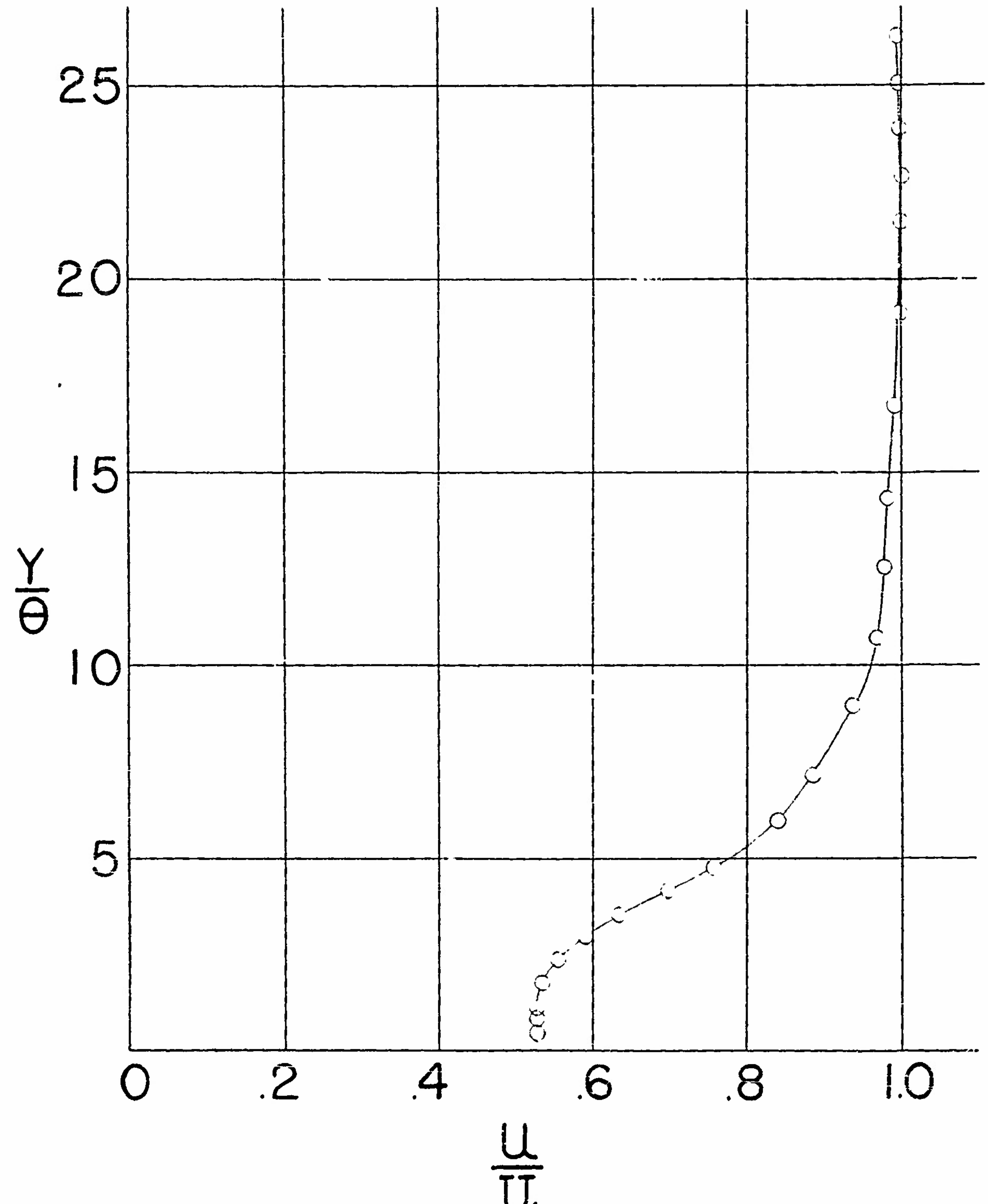

FIG. 13 VELOCITY PROFILE AT STATION -6

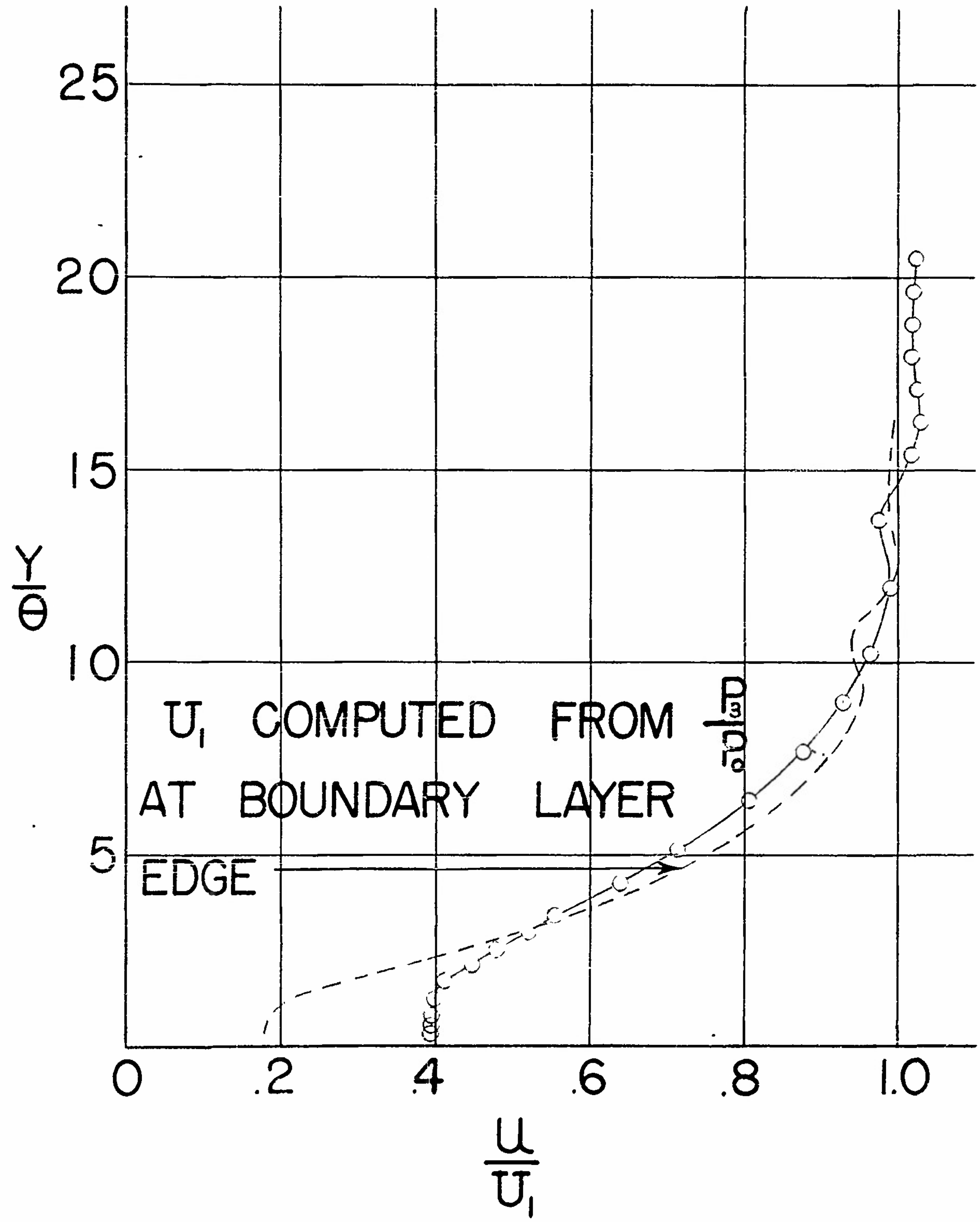

FIG. 14 VELOCITY PROFILE AT STATION –5

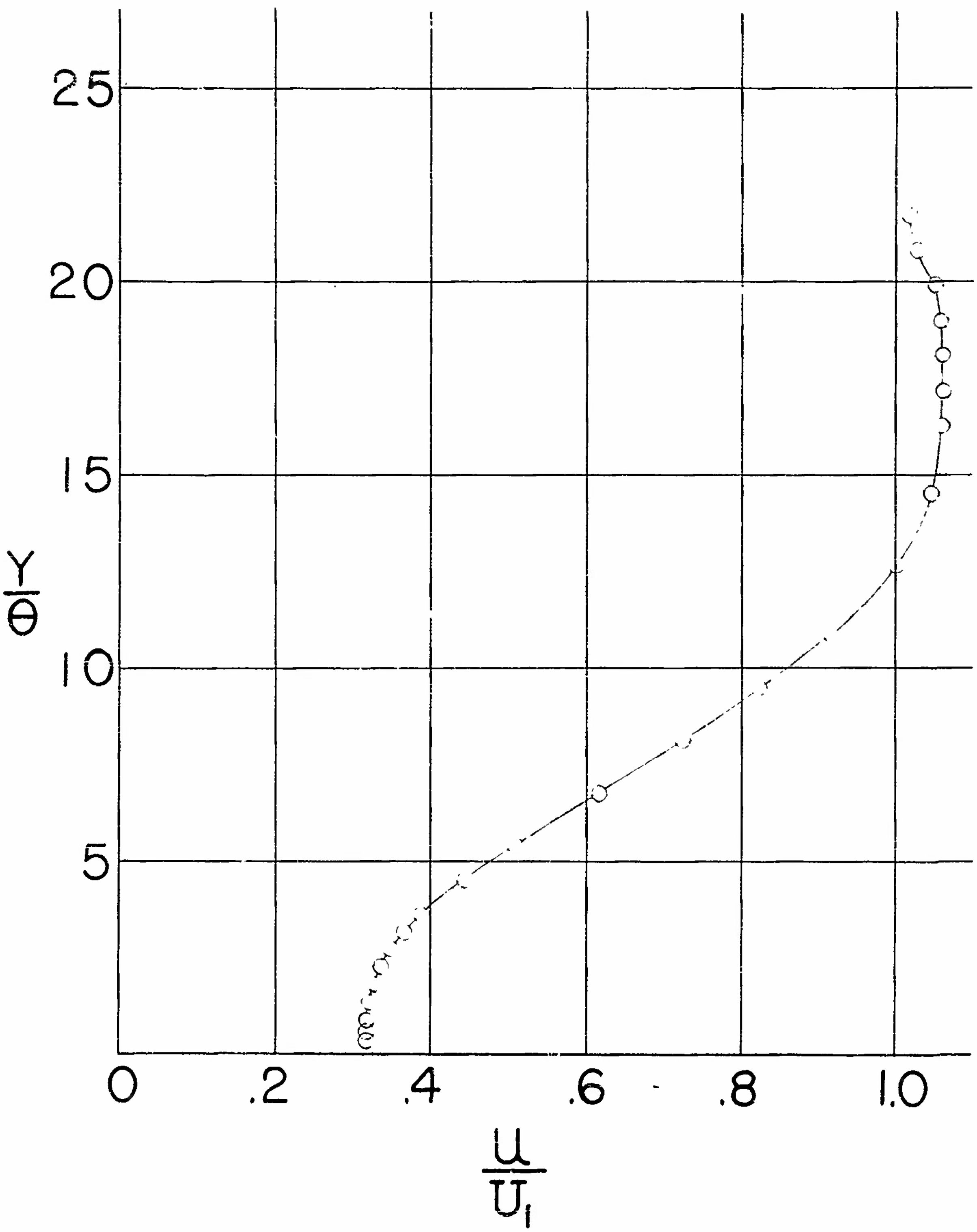

FIG. 15 VELOCITY PROFILE AT STATION -.3

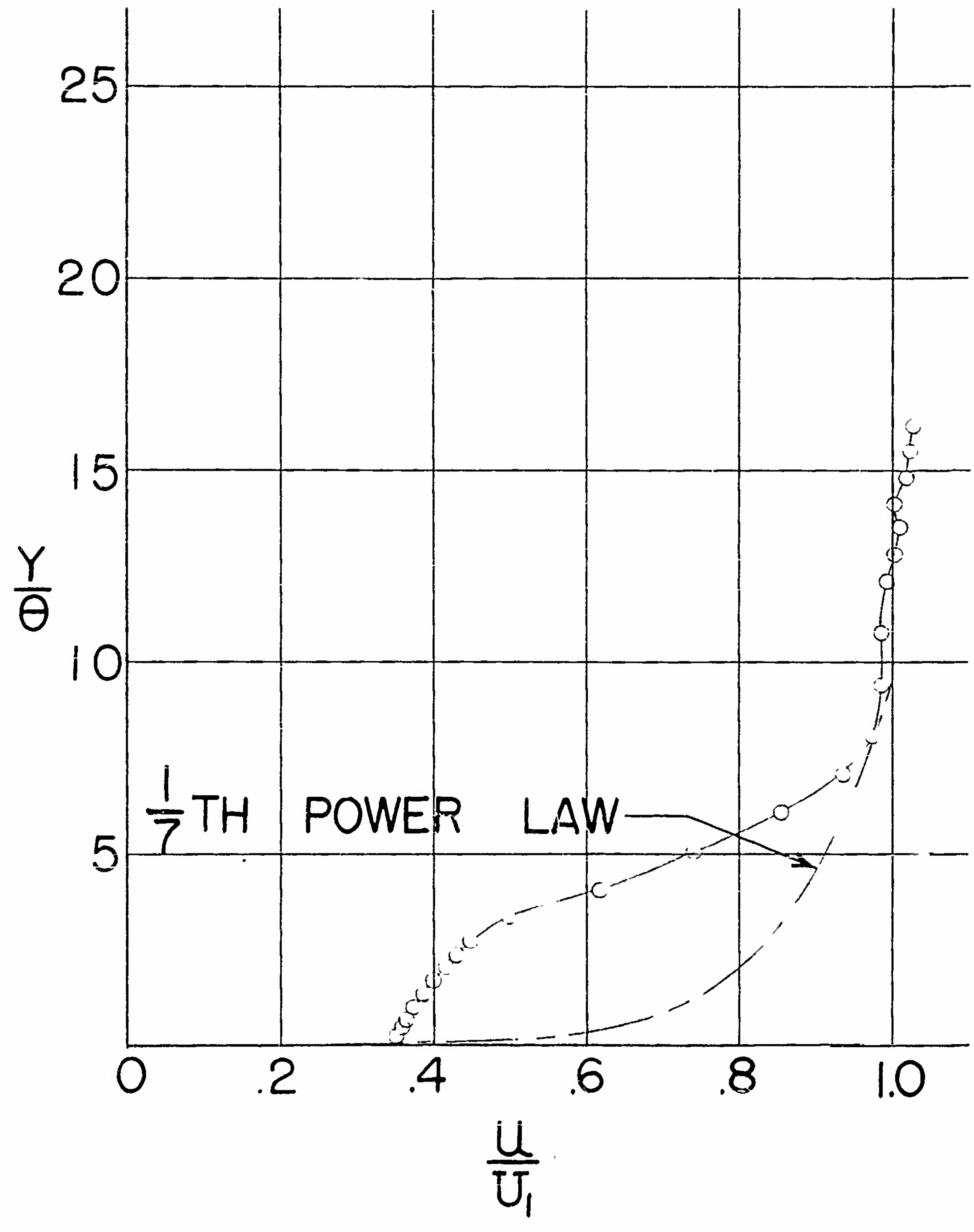

FIG. 16 VELOCITY PROFILE AT STATION -.1

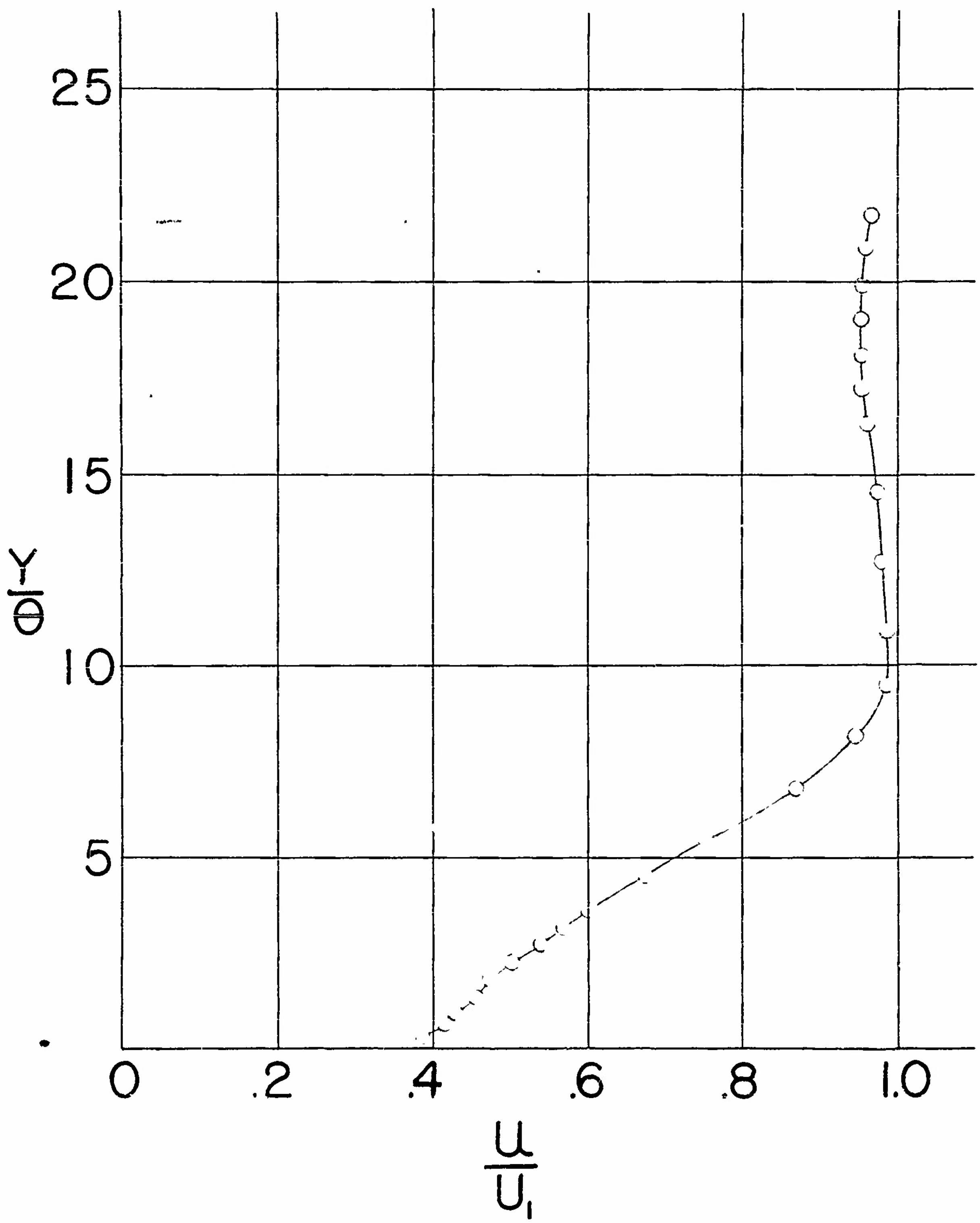

FIG. 17 VELOCITY PROFILE AT STATION +.1

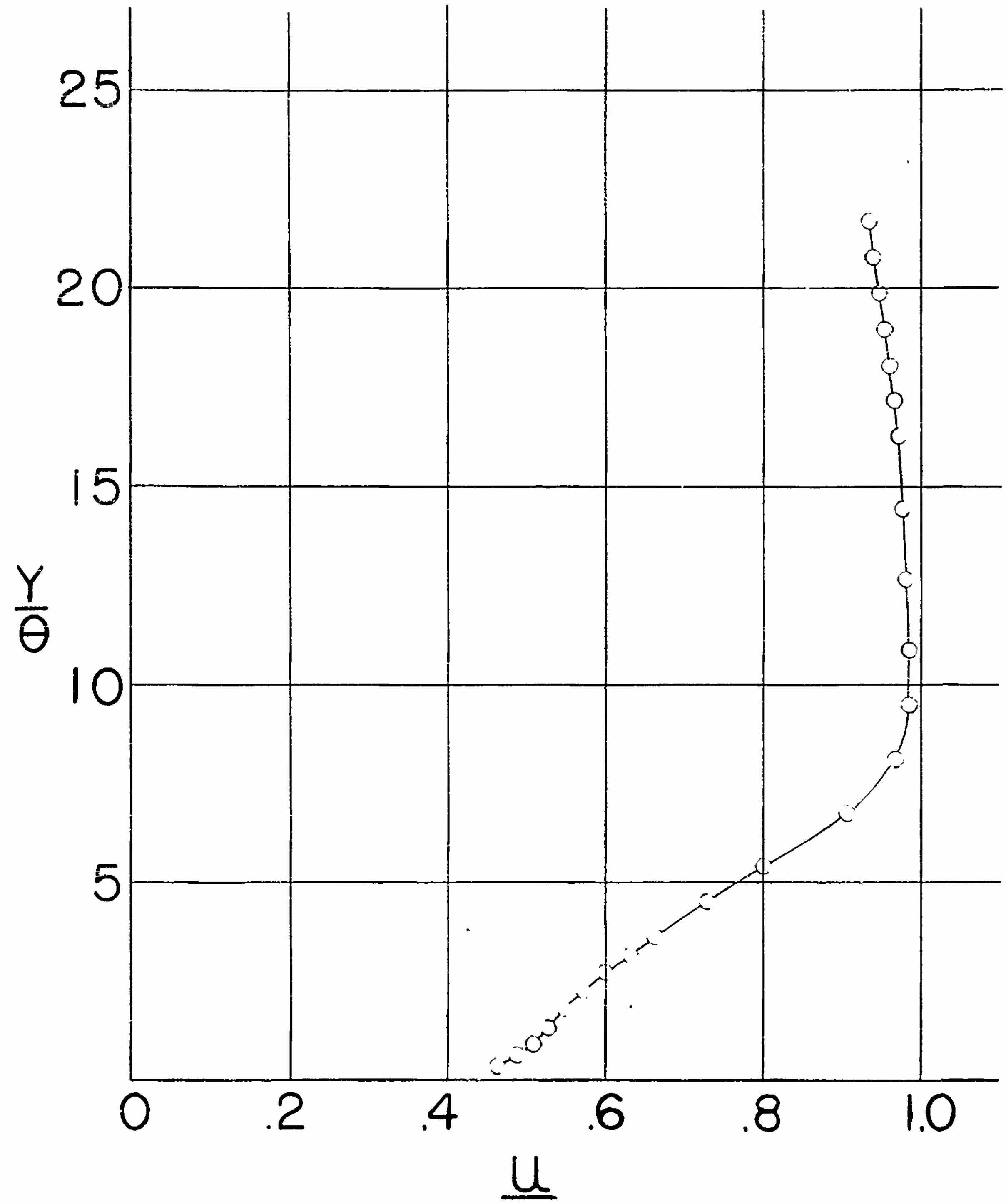

FIG. 18 VELOCITY PROFILE AT STATION +.3

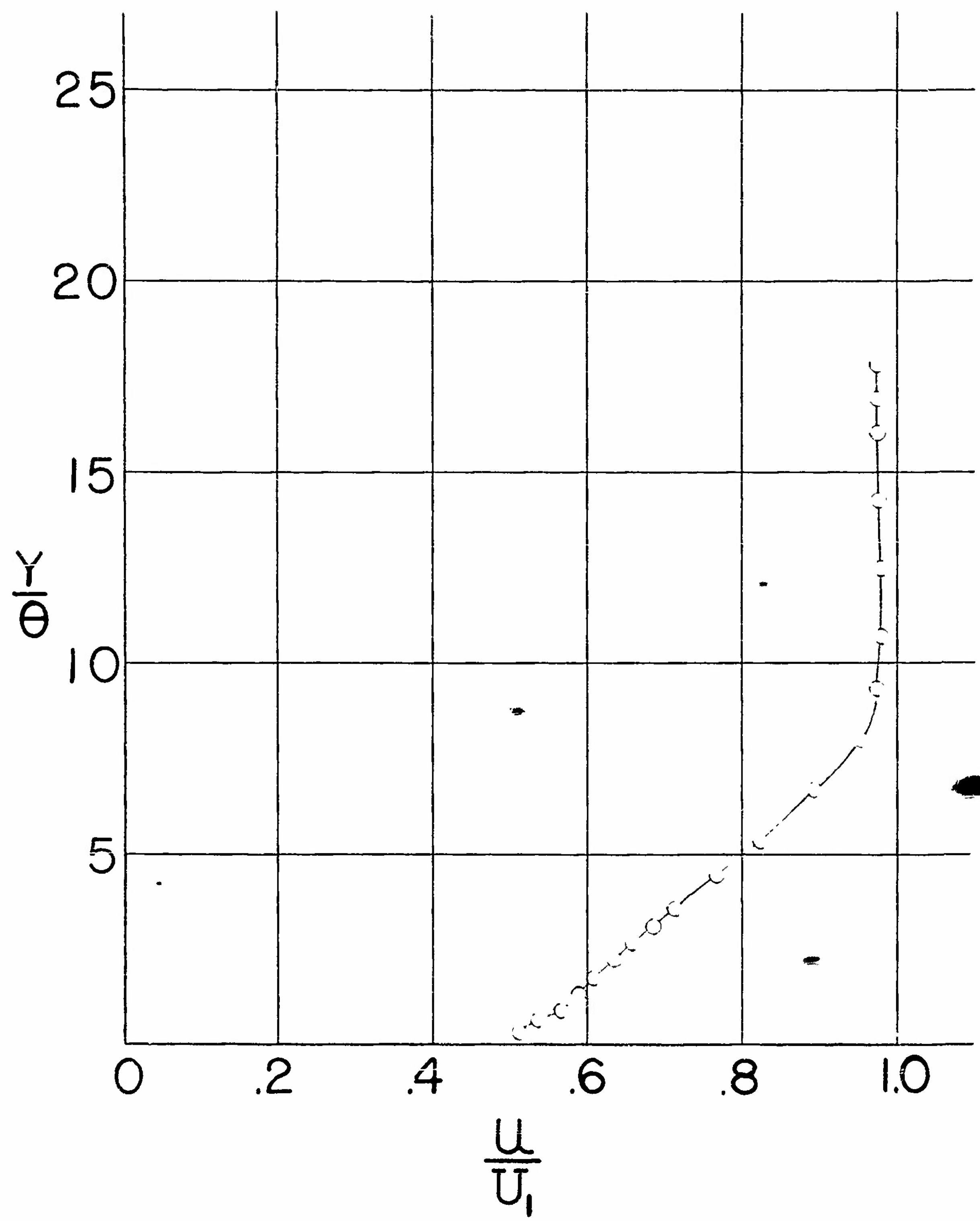

FIG. 19 VELOCITY PROFILE AT STATION +.5

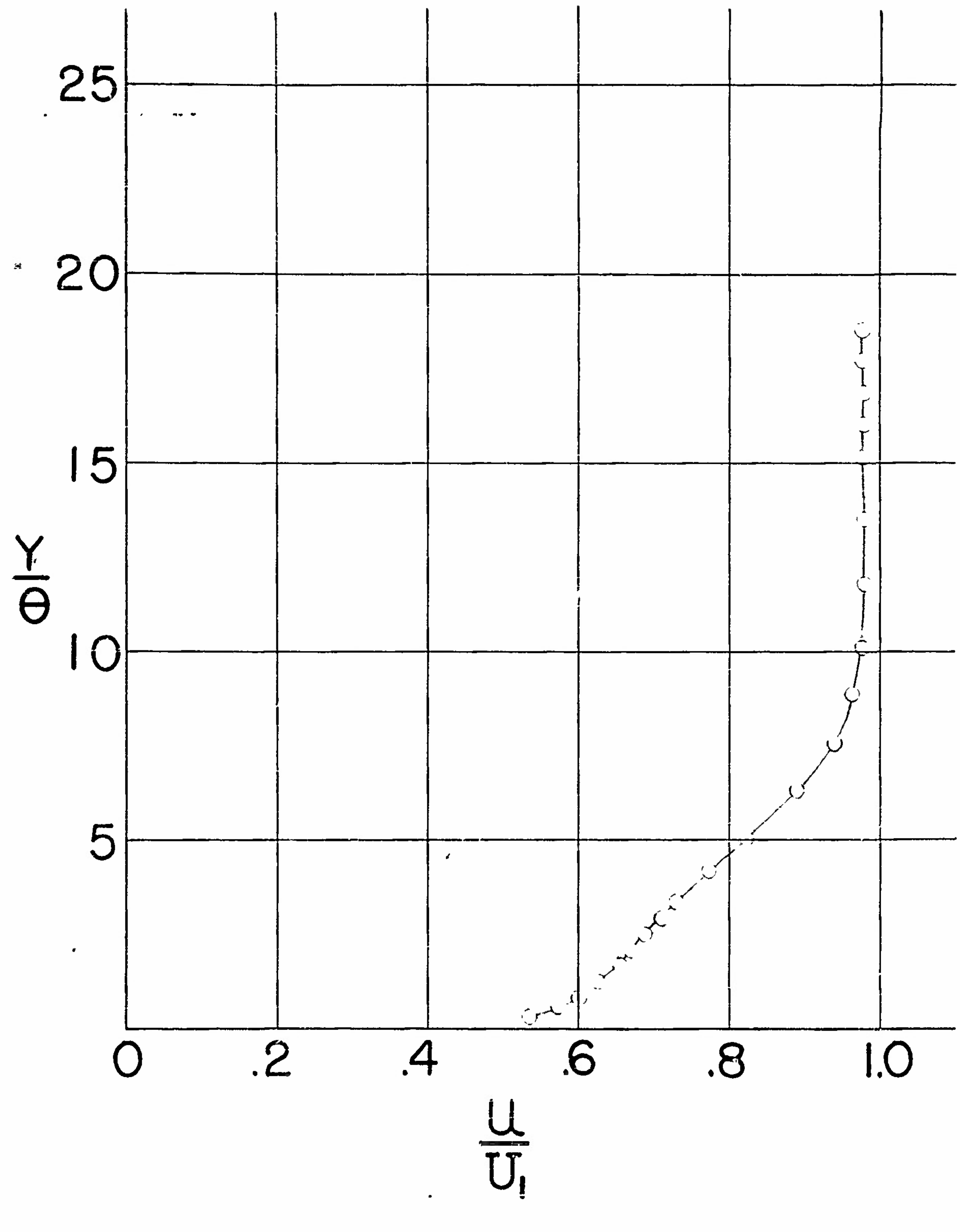

FIG. 20 VELOCITY PROFILE AT STATION +.7

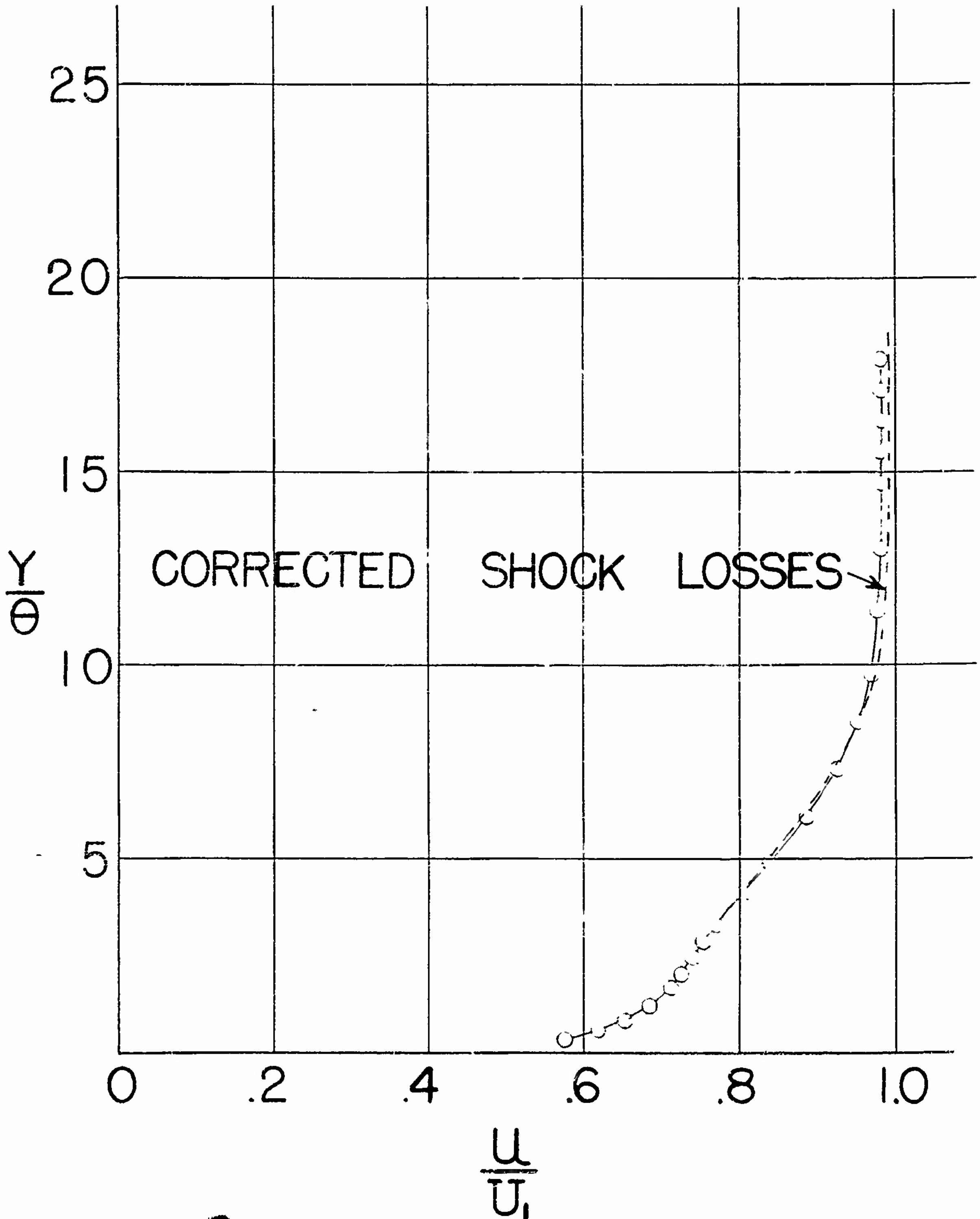

FIG. 21 VELOCITY PROFILE AT STATION +1.0

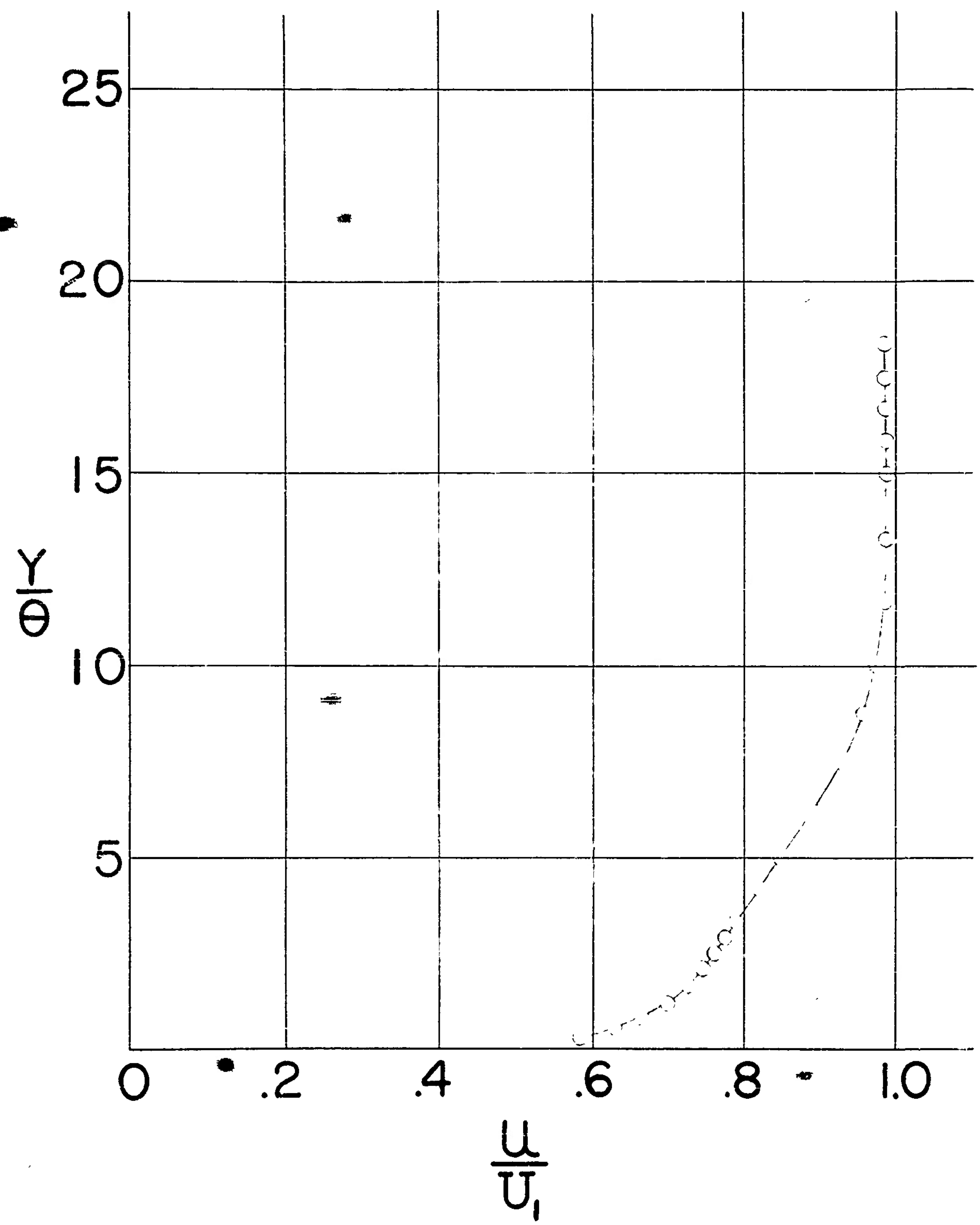

FIG. 22 VELOCITY PROFILE AT STATION +1.3

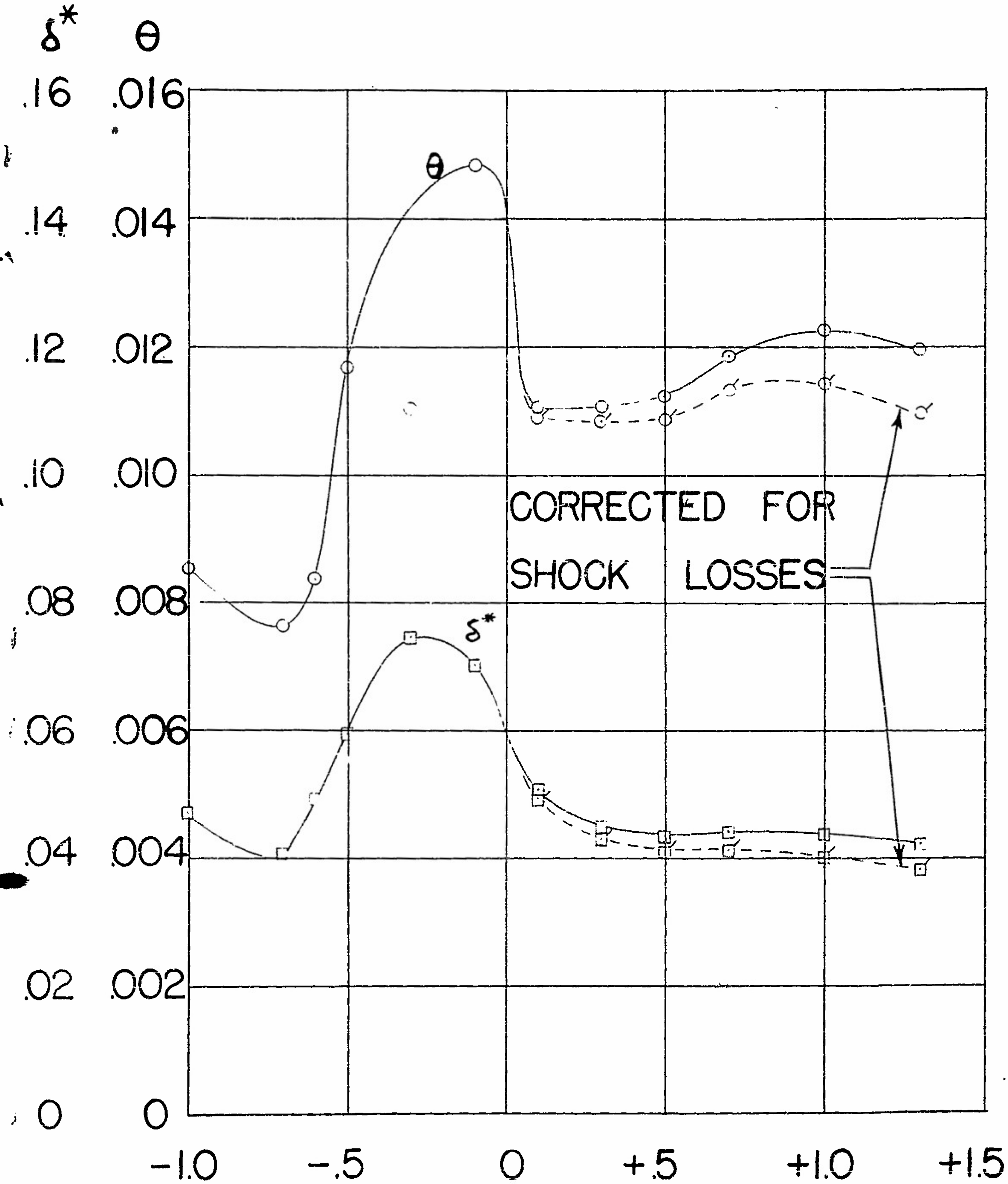

FIG. 23 VARIATION OF δ^* & θ THROUGH INTERACTION

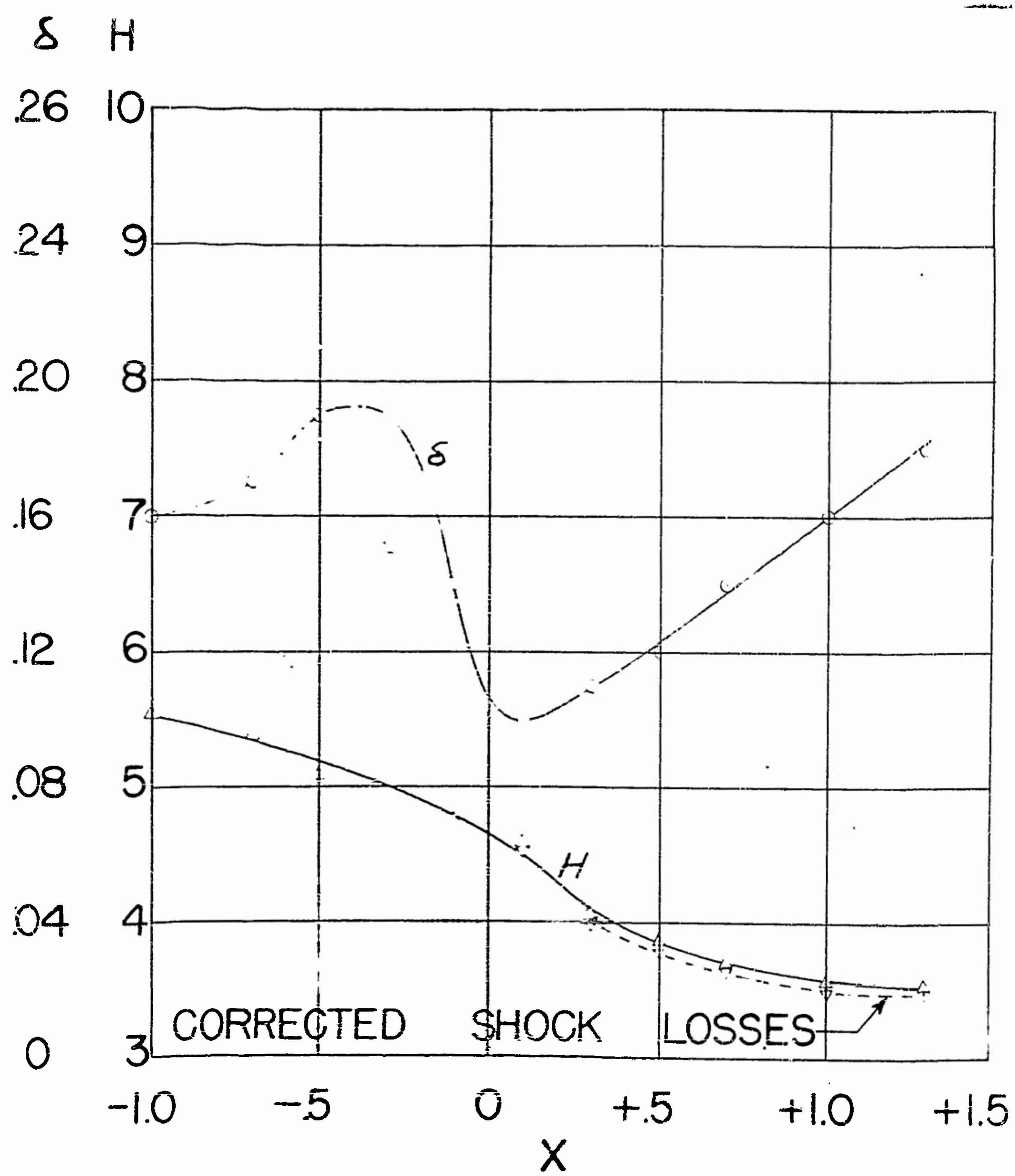

FIG. 24 VARIATION OF δ & H
THROUGH INTERACTION